

CHAPTER II

THEORETICAL BACKGROUND AND LITERATURE REVIEW

2.1 Silk Sericin

2.1.1 Overview of Silk Sericin

Silk, a natural protein fiber has been widely use in textile industries because of its mechanical properties and luster. Most commercial silk produced by mulberry silk worm, *Bombyx mori* belongs to Bombycidae family. The formation of silk cocoon composed of two major proteins named fibroin and sericin. Fibroin is the core protein constituted over 70% of cocoon and surrounding by sericin the “glue like” protein constituted 20-30% of cocoon. Sericin must be removed from fibroin during raw silk manufacturing by degumming process and usually discarded in silk waste water. (Kundu *et al.*,2008)

Sericin is hydrophilic protein containing 18 amino acids and most of which have strong polar side groups. The hydrophilicity of sericin comes from high amino acid serine content. Its molecular weight ranges widely from 10 to over 300 kDa. Sericin structure mainly occurs in amorphous random coil and less β -sheet structure with 63% and 35%, respectively (Kunda *et al.*, 2008, Zhang, 2002). It has sol-gel property since the random coil structure is soluble in water and when the temperature is lower the random coil structure turn to β -sheet structure resulting in gel formation (Padamwar *et al.*, 2004).

Vaithanomsat *et al.*, 2008 studied on the separation of sericin from silk waste water derived from silk manufacturer in Thailand. They determined the amino acid composition in sericin which is extracted from waste water compared with sericin extracted by hot water and sericin raw material as shown in Table 2.1.

Table 2.1 Amino acid composition in degumming solution compared with reference sericin (Vaithanomsat *et al.*, 2008)

Amino acid	Percent of gram amino acid in 100 g protein		
	Sericin raw material	Degumming solution ^a	Hot water-soluble sericin ^b
Aspartic acid	15.74	14.95	17.97
Serine	31.99	38.81	28.00
Glutamic acid	6.28	3.93	6.25
Glycine	14.20	14.45	16.29
Histidine	1.49	Not detected	1.32
Arginine	4.29	3.27	3.52
Threonine	7.73	7.79	7.78
Alanine	4.85	5.13	5.20
Proline	0.71	0.47	Not detected
Cytine	0.20	Not detected	0.69
Tyrosine	3.01	2.44	2.87
Valine	3.30	3.33	3.77
Methionine	Not detect	Not detected	Not detected
Lysine	4.17	3.12	3.72
Isoleucine	0.72	0.77	0.79
Leucine	0.96	1.18	1.21
Phenylalanine	0.37	0.34	0.64

^a From laboratory analysis

^b From reference

2.1.2 Degumming Process

In silk manufacturing, sericin is separated from fibroin by degumming process which based on solubility of sericin. There are several methods to remove sericin such as using hot water, acid solution, alkaline solution, and enzymes. Degumming by heat or heat under pressure has an advantage because an obtained sericin is no impurity. Using acid to remove sericin is more hazardous than using

alkaline. Most silk industries use extraction with soaps and detergents since it is a simple process compared with other processes (Aramwit *et al.*, 2012). Padamwar *et al.* (2004) reviewed many methods to degumming sericin. They reported that most of sericin was removed by autoclave under pressure of 600-700 mmHg (0.8-0.9 atm) for one and half hour and the satisfying yield was obtained from autoclaving at 105°C for 30 min with good gelling property and yield.

To recovery sericin from the degumming water to obtain sericin powder has been carried out by several methods such as freeze drying, spray drying, membrane filtration, enzymatic hydrolysis, and precipitation by ethanol (Aramwit *et al.*, 2012).

Vaithanomsat *et al.* (2008) studied on the methods to recover sericin compared between tray-drying and freeze-drying. They suggested that both drying methods gave the similar yield of recovered sericin powder with the similar composition excepted water solubility. The freeze-dried sericin was completely soluble in water but tray-dried sericin was dissolved only 96.28% in water. Hence, the heating process of tray-drying denatured protein in sericin resulting in the formation of thin film on the surface of the sericin solution during tested for water solubility. Therefore, they suggested using freeze-drying to dry sericin in the other experiment.

2.1.3 Application of Sericin

The application of sericin widely ranges from cosmetics to biomedical products. Due to its protein nature which is sensitive to proteolytic enzymes in the human body and digestible made sericin is biocompatible and biodegradable materials (Padamwar *et al.*, 2004). Because of high polar amino acid which consists of polar side chain such as hydroxyl, carboxyl, and amino groups made it easy to cross-link, copolymerize and blend with other polymer to improve the biodegradable property (Dash *et al.*, 2009).

Low molecular weight sericin is used in cosmetics for skin, hair, and nails. Sericin enhances skin elasticity, anti-winkle, and anti-aging effect. In the gel form, it has the moisturizing property thus it always used in lotion and cream. Moreover, sericin is used in nail cosmetics to prevent nail brittleness and shampoo for cleaning hair. In medical and pharmaceutical applications, sericin has been used as

antioxidants, anticancer drug, wound dressing, drug delivery, and film or hydrogel for tissue engineering etc. (Kundu *et al.*, 2008).

Sarovart *et al.* (2003) studied in the use of sericin in order to enhance the antioxidant, antifungal, and antimicrobial properties of indoor air filters by coating the filters with sericin in three different species of Thai cocoon: Nang Noi, Dok bua and Jul. From FTIR spectra as shown in Figure 2.1, sericin Dok Bua had highest absorbance and Jul had lowest absorbance indicated that sericin Dok Bua and Nang Noi have 18 amino acids and sericin Jul has only 14 amino acids. Furthermore, they found that as increased the concentration of sericin, the antioxidant, antifungal, and antibacterial efficiency in *Micrococcus* type increased and the efficiency was different in different species.

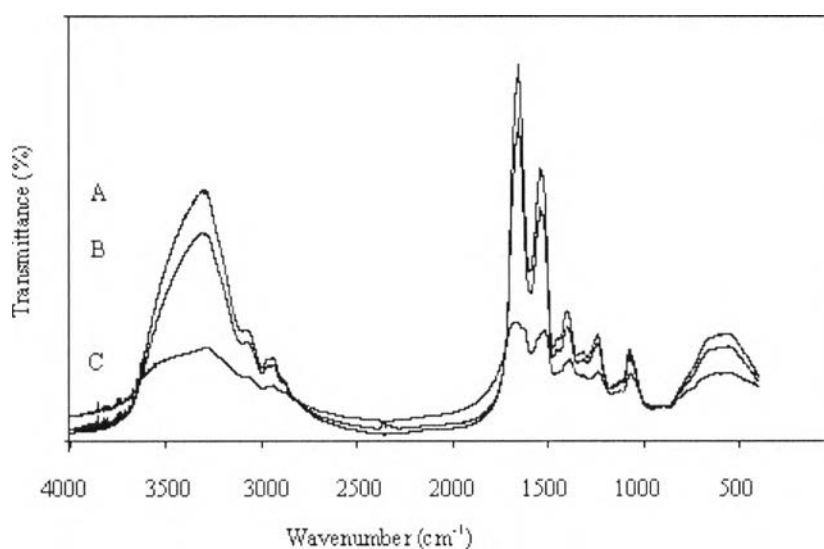


Figure 2.1 FTIR spectra of (A) Sericin Dok-Bua, (B) Sericin Nang-Noi, (C) Sericin Jul (Sarovat *et al.*, 2003).

Sericin has been studied in the form of porous material for biodegradable purpose and also for medical application. Porous structure of sericin via freeze-drying was investigated by Tao *et al.* (2005). They studied the effect of temperature and concentration of sericin solution on the structure and properties of porous material. Sericin was extracted from silk cocoon to obtain sericin solution with the concentration of 1.1% by weight and diluted to 0.7% and 0.3% by deionized water.

The porous sericin were prepared via freeze-drying process by using Poly(ethylene glycol) diglycidyl ether as a crosslink agent. The morphology of porous sericin is shown in Figure 2.2. They found that the decrease of freezing temperature and increase of sericin concentration result in the decrease of pore size and porosity but pore density was increased. The XRD curves indicated the main structure of porous sericin was amorphous and contained a few content of β -sheet and in the cross-linked sample the β -sheet structure was increased.

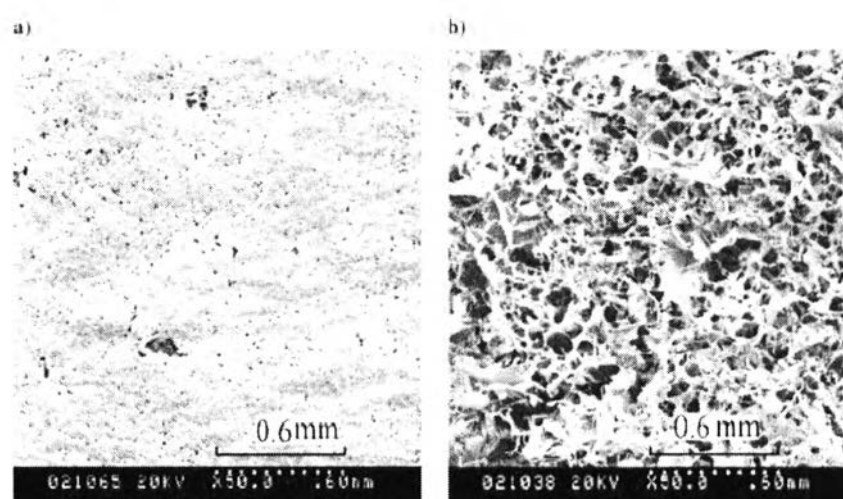


Figure 2.2 Scanning electron microscope (SEM) photographs of porous sericin material's surface (a) top-surface; (b) under-surface (Tao *et al.*, 2005).

2.2 Poly(lactic acid), PLA

2.2.1 Overview of PLA

PLA is the most widely used biopolymer-based packaging material with the highest potential for a commercial majority scale production. PLA synthesized from lactic acid which is derived from renewable resources, such as corn or sugar beets (Garlotta, 2001, Gupta and Kumar, 2007 and Lim *et al.*, 2008). Structurally, PLA is a linear aliphatic polyester, which is a thermoplastic with high-strength, high-modulus, good processability, be completely biodegradable, compostable, and biocompatible, and therefore perfectly safe for the environment and for the food packaging application. PLA presents a medium water and oxygen permeability level

comparable to polystyrene (Auras, Harte, & Selke, 2004). In addition, PLA is safe and “Generally Recognized As Safe” (GRAS) for use in food packages (Conn *et al.*, 1995). However, its high polarity, brittleness, stiffness, noise, and low deformation at break limit its use. Considerable efforts have been made to improve the properties of PLA so as to compete with low-cost and flexible commodity polymers. These attempts were carried out either by modifying PLA with biocompatible plasticizers or by blending PLA with other polymers (Luckachan & Pillai, 2011).

Auras *et al.* (2004) reported that PLA films have better ultraviolet light barrier properties than low density polyethylene (LDPE), but they are slightly worse than those of cellophane, polystyrene (PS) and poly(ethylene terephthalate) (PET). PLA films have mechanical properties comparable to those of PET and better than those of PS. PLA also has lower melting and glass transition temperatures than PET and PS. The glass transition temperature of PLA changes with time. Humidity between 10 and 95% and storage temperatures of 5 to 40 °C do not have an effect on the transition temperature of PLA, which can be explained by its low water sorption values (i.e. <100 ppm at $A_w=1$). PLA seals well at temperatures below the melting temperature but an appreciable shrinking of the films has been noted when the material is sealed near its melting temperature. Solubility parameter predictions indicate that PLA will interact with nitrogen compounds, anhydrides and some alcohols and that it will not interact with aromatic hydrocarbons, ketones, esters, sulfur compounds or water. The CO_2 , O_2 and water permeability coefficients of PLA are lower than those of PS and higher than those of PET. Its barrier to ethyl acetate and D-limonene is comparable to PET. The amount of lactic acid and its derivatives that migrate to food simulant solutions from PLA is much lower than any of the current average dietary lactic acid intake values allowed by several governmental agencies. Thus, PLA is safe for use in fabricating articles for contact with food.

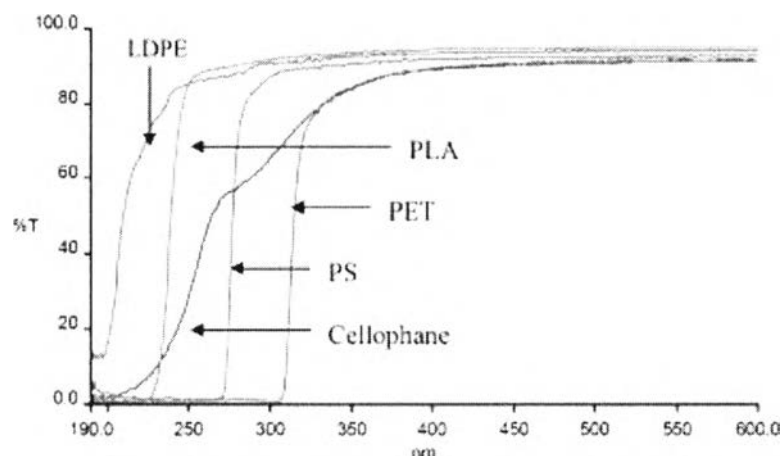


Figure 2.3 Percent transmission versus wavelength for PLA(98% L-lactide). PS, LDPE, PET and cellophane films. (PLA samples were obtained from Cargill Dow LLC).

Conn *et al.* (1994) reported that the calculated 0.0180 ppm dietary concentration of lactic acid from all proposed uses of PLA as an indirect food additive translates to not more than 0.054 mg/day/person. This represents less than 0.25% of the current intake of lactic acid from all sources of lactic acid added directly to foods. If the amount of lactic acid consumed as a natural component of several common foods is also considered, the very slight additional increment of lactic acid that would result from the proposed uses of PLA as an indirect food additive becomes even smaller. As a final comparison, the projected intake of lactic acid from PLA is approximately 700 times less than the estimated lactic acid intake of breast-fed infants.

There are many monomers which have been copolymerized with PLA to improve the weak properties of PLA. A polycondensation of lactic acid copolymerized with other monomers, produced low molecular weight copolymer. Monomers were used in polycondensation copolymerization such as D,L-mandelic acid and other α -hydroxy acids, etc. Moreover, ring-opening copolymerization of lactide monomer with cyclic monomer produced high molecular weight copolymer. Cyclic monomers were used in ring-opening copolymerization such as glycolide, trimethylene carbonate, ϵ -caprolactone, etc. (Sodergard, 2002).

In 2000, Hiki *et al.* studied L-lactide block copolymerization with hydroxyl-terminated [RS]-poly(3-hydroxybutyrate) ([RS]-PHB) by the catalyst of tin (II) octoate. They studied the effect of L-lactide and [RS]-PHB content from 44 to 69% and studied the effect of an increase of reaction temperature. The yield result of copolymers was very high and molecular weight was around 11,900-30,000 Da. The feed ratio of L-lactide affected to the molecular weight. The molecular weight distribution was very low. Furthermore, they studied on mechanical properties of block copolymerization of [RS]-PHB and L-lactide. The polymer film was made from the PLLA-[RS]-PHB-PLLA that gave the Young's modulus increase from 30 to 160 MPa when the composition of PLLA was increased. In contrast, the elongation at break was increased from 20 to 86% (Hiki *et al.*, 2000).

2.3 Clay Mineral – Sodium Bentonite

2.3.1 Overview of Bentonite Clay

The smectite clays are valuable minerals widely used in many applications. Smectite is the family name which includes sodium and calcium montmorillonites and the rock that composed dominantly of smectite minerals is generally called bentonite. (Murray, 1991)

Bentonite from the alternative of volcanoclastic or pyroclastic rock and it is composed of montmorillonite. (Karakaya *et al.*, 2011) Smectites are the three-layer clay mineral which composed of two silica tetrahedral sheets joined to a central octahedral sheet of either aluminum or magnesium hydroxide to form as a 2:1 layer or phyllosilicates. The layer thickness is around 1 nm and the lateral dimensions of these layers may vary from 30 nm to several microns or larger, depending on the particular layered silicate. Stacking of the layers leads to a regular van der Waals gap between the layers called the interlayer or gallery. There are some substitutions of Fe^{2+} and Mg^{2+} for Al^{3+} in the octahedral sheet and also some substitutions of Al^{3+} for Li^{1+} in the tetrahedral sheets. The substitution creates a negative charge imbalance which is about -0.66/unit cell. The net positive charge deficiency is balanced by exchangeable cation adsorbed between the unit layers and around the edges. If the

exchangeable cation is sodium, the specific mineral is sodium montmorillonite. (Murray, 1991, Ray *et al.*, 2003) Figure 2.4 shows the structure of 2:1 pylosilicates and Table 2.2 introduces the chemical formular and characteristic parameter of 2:1 pylosilicates.

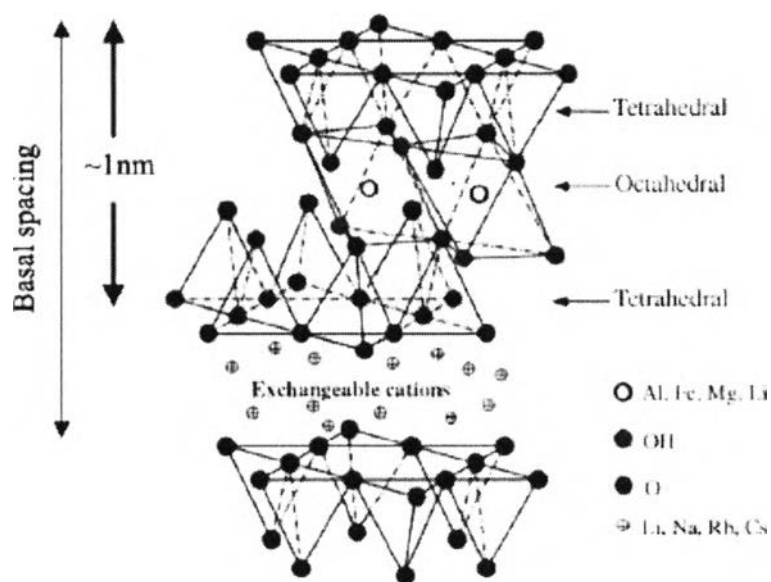


Figure 2.4 Structure of 2:1 pylosilicates (Ray *et al.*, 2003).

Table 2.2 Chemical formula and characteristic parameter of commonly used 2:1 phyllosilicates (Ray *et al.*, 2003)

2:1 phyllosilicates	Chemical formula	CEC (mequiv/100g)	Partical length (nm)
Montmorillonite	$M_x(Al_{4-x}Mg_x)Si_8O_{20}(OH)_4$	110	100-150
Hectorite	$M_x(Mg_{6-x}Li_x)Si_8O_{20}(OH)_4$	120	200-300
Saponite	$M_xMg_6(Si_{8-x}Al_x)Si_8O_{20}(OH)_4$	86.6	50-60

where M is monovalent cation and x is degree of isomorphous substitution (between 0.5 and 1.3)

Sodium montmorillonite which is the major component of sodium bentonite generally has one water layer in the interlayer position and the basal spacing is 12.2 Å. It is high-swelling when clay placed in water; it will expand up to 10 or more times than its dry volume. The cations and water layers can be replaced by polar organic molecules such as ethylene glycol, quaternary amine, polyalcohols, and others. This is an important property which can be translated into useful products. (Murray, 1991)

2.3.2 Polymer/Clay Nanocomposite

Layered silicate clay has a very high aspect ratio. A few weight percent of clay which are suitable for dispersed clay into the polymer matrix and created high surface area for polymer/clay interaction.

The structure of polymer/clay nanocomposites can be classified into three different types:

1. **Intercalated structure** which the insertion of a polymer matrix into the clays structure occurs only in a crystallographically regular fashion. Intercalated nanocomposites are normally interlayer by a few molecular layers of polymer.
2. **Flocculated structure** which is the same as intercalated nanocomposites but sometimes clay are flocculated because of hydroxylated edge–edge interaction of the silicate layers.
3. **Exfoliated structure** which the individual clay layers are separated in a continuous polymer matrix by an average distances depends on clay loading.

Clays usually are in the intercalated form more than exfoliated form. However, the exfoliated structure is more required because it gives the superior reinforcing efficiency. (Ray *et al.*, 2003, Pojanavaraphan *et al.*,2008)

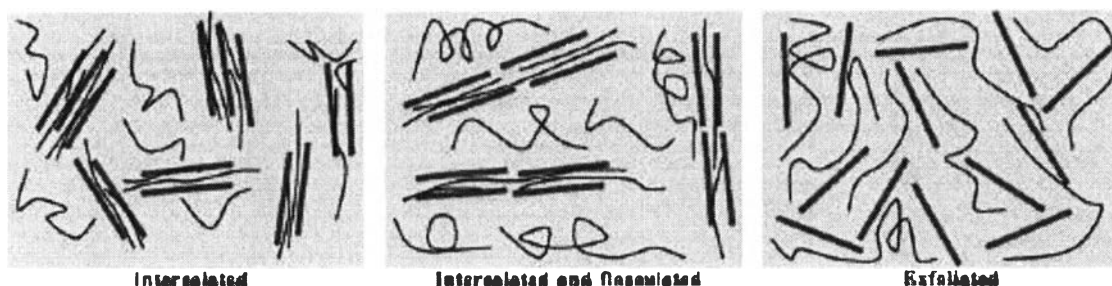


Figure 2.5 Schematically illustration of three different types of achievable polymer/clay nanocomposites (Ray *et al.*, 2003).

2.3.3 Clay Aerogel

Aerogel was first described in 1932 by Kistler. Aerogel is used to express the inorganic gels which the liquid was replaced with gas without collapsing the solid network with the bulk density in the range of 0.01-0.1 g/cm³. Aerogel has a very high relative and specific pore volume depend on the nature of solid materials. Normally, the relative pore volume of aerogel is about 90% in the study of silica aerogels but may be lower in other type of aerogels. (Aegerter *et al.*, 2011, Bandi *et al.*, 2005)

Layered clays can be rearranged to house of cards like aerogels structure by freeze-drying process. Mackenzie and Call found the preparation of montmorillonite clay aerogels by freeze-drying clay hydrogels resulted in fibrous montmorillonite structures. The clay aerogel has rigidity, but poor thermal stability at 110°C. In 1967, Van Olphen described that the house of card structure of clay aerogel was occurred because of the opposite edge and face electrostatic charge. The faces have negative charges on siloxane surface and the edges have positive charges of alumina sheet resulting in the charge attraction. When clays are freezed, the ice crystals are growing and push the particles aside to encourage the parallel alignment. (Pojanavaraphanet *et al.*, 2008, Bandi, 2006)

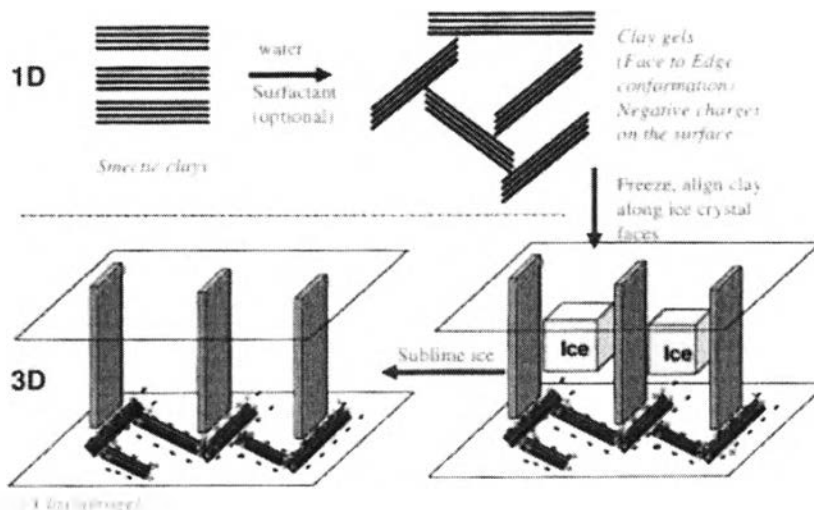


Figure 2.6 Synthesis of clay aerogels (Somlai *et al.*2006).

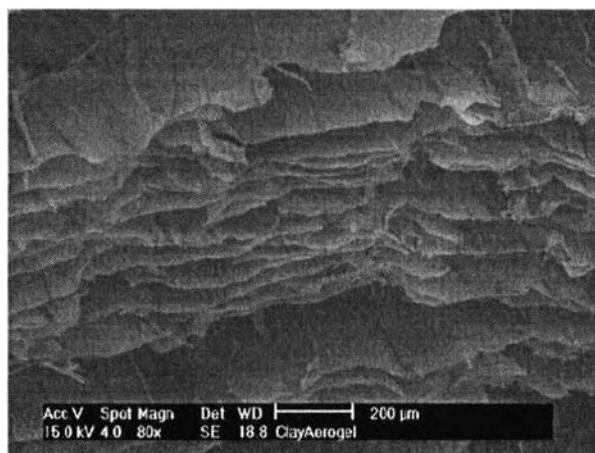


Figure 2.7 SEM image of freeze dried clay to form Clay Aerogel (“house of card” sheet-like structure) super gallery spacing $\sim 200 \mu\text{m}$. (Bandi, 2006).

Neat clay aerogels are relative fragile which exhibit low mechanical properties thus they are easy to break under low stress level. To overcome this problem, the combination of polymeric materials or fibers into the clay aerogels are required. The incorporation polymer into clay aerogels can improve mechanical properties, produce the form-like structure and also expanded the range of applications. Many polymer/clay aerogel composites were investigated such as

natural rubber/clay aerogel composite, PNIPAM/clay aerogel composite, silk fibroin/clay aerogel biocomposite, and casein/clay aerogel biocomposite. (Pojanavaraphan *et al.*, 2008, Pojanavaraphan *et al.*, 2010, Bandi *et al.*, 2005, Finlay *et al.*, 2008)

Somlai *et al.* (2006) studied on the organically-modified clay aerogel by using sodium-exchanged (PGW), 12-aminolauric acid exchanged (ALA), and octadecyltrimethyl quaternary amine salt (EXT) exchanged montmorillonite. The organoclay was dispersed in water, then, mixed with HCl and purified Maleic Anhydride with Triethylene Glycol (MATEG) which is a surfactant. Then the mixture were frozen at -80°C and evacuated for 36 h in freeze-dryer. After freezing the clay suspension for 1 h, the highly ordered ice-clay patterns were observed. After vacuum for 48 h, a soft stacked layer and highly ordered with a like sheet textured was produced with interlayer voids which were approximately 100-200 microns. They introduced the morphology formation of clay aerogel according to Nakazawa *et al.*'s research as shown in Figure 8. They reported the process parameter such as shear rate, surfactants and freezing conditions which were affected to the formation of aerogel structure. Moreover, the concentration of clay in water was important because the concentration less than or equal 0.7 wt% did not form aerogel structure and the concentration above 2.9 wt% were viscous and difficult to blend. WAXD result indicated that surfactant was intercalated into clay due to the increasing of d_{001} spacing.

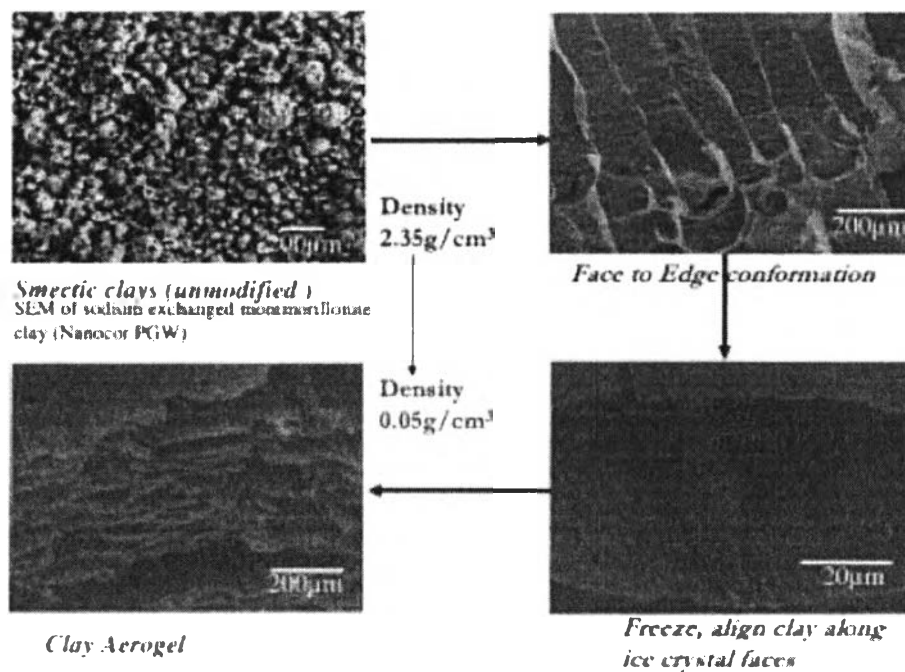


Figure 2.8 The morphology formation of clay aerogel (Somlai *et al.*, 2005).

In 2008, Pojanavaraphan *et al.* invented the pre vulcanized natural rubber latex/clay aerogel nanocomposites using pristine clay (Na-montmorillonite). The Na-MMT content was varied in 1-3 phr in order to study the effect of clay in NR Matrix. The pre vulcanized NR latex was mixed with the dispersion of pristine clay followed by stirring for 30 min at room temperature. Then the mixture was frozen immediately in cylindrical glass shells at liquid nitrogen temperature and was sublimed ice in freeze-dryer maintained at -54°C in vacuum for 36 h. The samples were vulcanized with two methods including thermal curing and microwave curing. They found that the neat Na-MMT aerogel was not an exfoliated structure but only appeared as clay bundle. In case of NR/MMT, the XRD patterns showed the increasing of d_{001} spacing indicated that rubber intercalated in the clay platelets. In addition, the nanocomposite with 3 phr MMT had no diffraction peak, which indicated the exfoliation of clay platelets. In case of nanocomposite with 1 and 2 phr MMT, showed the clay content was not enough to form the aerogel structure; on the other hand, the aerogel structure begin to formed in NR/3MMT. The SEM micrograph of NR/3MMT is shown in Figure 2.9.

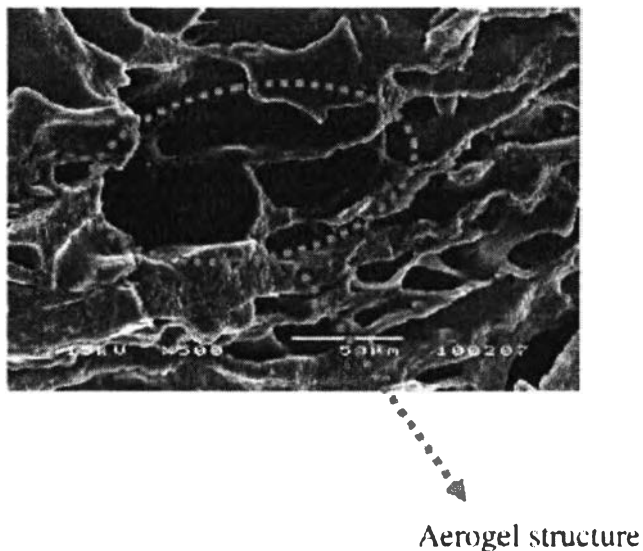


Figure 2.9 SEM micrograph of NR/3MMT (Pojanavaraphan *et al.*).

Furthermore, hardness of the aerogel increased with the increasing of MMT content. In this work, it has the interesting point in the thermogravimetric analysis. They found that the onset and peak of degradation temperatures of NR were slightly decreased with increasing of MMT content due to the acceleration in the thermal degradation of NR by Fe^{3+} isomorphously substituted in the octahedral sheet of Na-MMT clay.

Afterward, Pojanavaraphan *et al.* (2010) also studied on the mechanical, rheological and swelling behavior of natural rubber/montmorillonite aerogels by freeze-drying. The pre Vulcanization NR latex contained 60% NR mass was diluted to 30% NR mass and slowly mixed with Na-MMT dispersion in different contents. The mixture was frozen in cylindrical glass vials at -80°C . The frozen samples were transferred to freeze-dryer with condenser temperature at -108°C for 3 days. The XRD patterns indicated that the composites were intercalated because of the increasing of basal spacing. SEM micrographs showed that only the composites with 5 and 7 phr Na-MMT was observed the regular layered morphology and completely covered by NR layers. They suggested that Na-MMT requires at least 2% MMT to achieve the aerogels structure. The swelling behavior of aerogel determined by the equilibrium solvent uptake showed that the equilibrium solvent uptake increased with increasing of Na-MMT content and decreasing of cross-linking density. From

the compression test and DMA indicated that the mechanical properties increase with the increasing of Na-MMT content. The composites were stiff due to the reinforcing effect of Na-MMT and the present of voids in the composites contained 7 phr of Na-MMT.

Table 2.3 The initial modulus and reinforcing efficiency of nanocomposites (Pojanavaraphan *et al.*, 2010)

Samples	Initial modulus (kPa)	Reinforcing efficiency (%)
PNR	17.3 ± 6.3	-
PNR/M1	19.3 ± 7.1	14.6
PNR/M3	23.0 ± 4.5	29.1
PNR/M5	22.5 ± 4.0	22.7
PNR/M7	35.4 ± 11.8	80.7

Liu *et al.* (2011) prepared the chitosan/xanthan gum/montmorillonite macroporous by using freeze-drying method. The mixture of chitosan and xanthan gum was mixed with suspension unmodified Na-MMT clay. They investigated the effect of the freezing rate and freezing process; immersion freezing and contact freezing to the formation of the macroporous foams. They found that the addition of Na-MMT exhibited the greater rigidity and increased the mechanical strength of freeze-dried foams when compared with the freeze-dried foam from only chitosan/xanthan gum. The hardness was increased when incorporated Na-MMT into the nanocomposite and the highest hardness value was observed in sample that prepared at slow freezing rate with the presence of Na-MMT as shown in Figure 2.10.

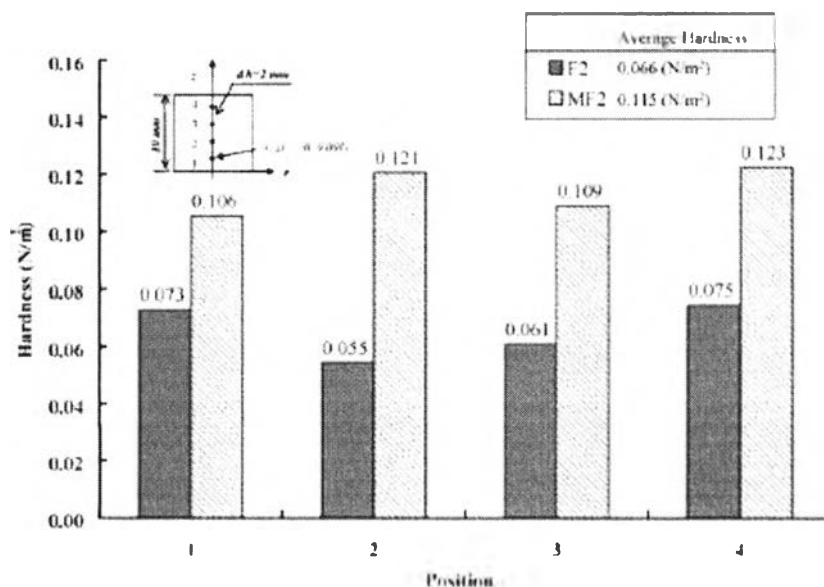


Figure 2.10 Hardness results for samples prepared via slow freezing rate: F2 = chitosan/xanthan gum and MF2 = chitosan/xanthan gum/Na-MMT.

The SEM micrograph showed the well interconnect pores occurred in all samples. The addition of Na-MMT slightly increased the pore size; however the pore size was surely depended on the freezing front velocity.

Pojanavaraphan *et al.* (2010) developed the form liked materials based on casein and Na-MMT clay using DL-glyceraldehyde (GC) as a crosslinking agent. The foam liked structure was produced by freeze-drying process. The Na-MMT aqueous suspension was slowing added into casein-GC solution with the GC to casein ratio was 1:20. The mixture was frozen at -80°C and freeze-dried in lyophilizer for 4 days and post cured at 80°C for 24 h. They suggested that GC was chosen because it is non-toxicity when compared with glutaraldehyde (GT), the common aldehyde used to crosslink protein. However, GC is low reactivity so it requires post curing at high temperature. The incorporation of GC resulted in the higher compressive modulus and toughness. Adding of 5 wt% GC increased compressive modulus and toughness at 30% stain from 3900 to 5600 and 58 to 72 kPa, respectively. Adding GC was also slightly increased the thermal stability. The higher casein content gave higher mechanical and thermal properties due to the

continuous architecture in the layers were connected by polymer. Moreover, the biodegradation study indicated that the casein and casein/Na-MMT aerogel exhibited low degradation rate compared with the degradation behavior of wheat starch since the house of card structure increased the time for degradation due to the microorganism was more difficult to approach the internal region.

2.4 Plasma Treatment and Acrylic Acid

Plasma is chemically active media. Depending on the way it is activated and its working power, it can generate low or very high temperatures and is referred correspondingly as cold or thermal plasma. This wide temperature range enables various applications for plasma technologies: surface coatings, waste destruction, gas treatments, chemical synthesis, or machining. Plasma consists of electrons, ions and neutrals which are in fundamental and excited states. From a macroscopic point of view, plasma is electrically neutral. However, it contains free charge carriers and is electrically conductive. A plasma is created by applying energy to a gas (Conrads *et al.*, 2000) in order to reorganize the electronic structure of the species (atoms, molecules) and to produce excited species and ions. This energy can be thermal, or carried by either an electric current or electromagnetic radiations.

Acrylic acid is commercially available in two grades: technical grade (94%) for esterification, and glacial grade (98-99.5% by weight and a maximum of 0.3% water by weight) for production of water-soluble resins. Acrylic acid polymerizes easily when exposed to heat, light or metals, and so a polymerization inhibitor is added to commercial acrylic acid to prevent the strong exothermic polymerization. Acrylic acid reacts readily with free radicals and electrophilic or nucleophilic agents. It may polymerize in the presence of acids (sulfuric acid, chlorosulfonic acid), alkalis (ammonium hydroxide), amines (ethylenediamine, ethyleneimine, 2- aminoethanol), iron salts, elevated temperature, light, peroxides, and other compounds that form peroxides or free radicals. In the absence of inhibitor, peroxides are formed when oxygen is sparged into acrylic acid. The presence of oxygen is required for the effective function stabilizer. Acrylic acid must never be handled under an inert atmosphere.

Ren *et al.* (2006) studied the ability of graft co-polymerization of acrylic acid (AAc) onto the linen surface by DBD treatment in air. Induced by DBD in air, AAc has been successfully grafted onto linen surface and this is verified by the methods of DTA, SEM, FTIR-ATR and visible absorption spectroscopy. The treatment of plasma produced by DBD in air can form radical sites on linen surface and the radical sites will work as the initiators for the graft co-polymerization of AAc onto linen surface. An optimal plasma treatment time of 30 s has been obtained for the maximum grafting degree in their study. Prolonged treatment time will lead to the decrease of the grafting degree instead. However, when grafting time reaches 140 min, graft co-polymerization will get saturation. An optimal grafting temperature of 70 °C and grafting solution concentration of 60% are also obtained in the experiment. This can be explained by the fact that, in the process of graft, the reactions of graft co-polymerization and homopolymerization compete with each other.

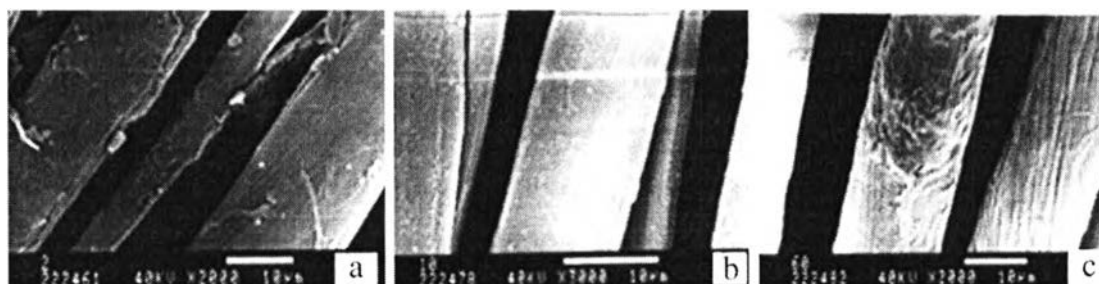


Figure 2.11 SEM picture of the (a): original, (b): air-DBD treated and (c): DBD and graft treated linen samples. The DBD-treatment time is 30 s.

Liam *et al.* (1996) prepared plasma polymers of acrylic (propenoic) acid and propanoic acid from inductively coupled, radio-frequency-induced plasmas excited in vapors of the starting materials. Based on a mass spectrometric study of the plasma polymerization of acrylic acid at low P , they have proposed that polymerization takes place predominantly through the carbon-carbon double bond and this gives rise to the high levels of functionalization as measured by XPS as shown in figure 2.12. Moreover, the deposition rate of acrylic acid was 5 times that

of propanoic acid. At low P , in plasmas of acrylic acid, the mechanism of polymerization resembles that of cationic chain growth. At higher P , free-radical reactions are likely to assume and the selectivity in the reaction site has been lost. The spectroscopic data reveal some loss of carboxyl from the monomer, presumably as CO_2 , which is then pumped away. The carboxyl retained in the product is present as both acid and ester. This implies direct incorporation of oxygen within the polymer network. The increase in the ion ratio m/z 73/71 can be taken to indicate a greater degree of branching, giving a higher concentration of end groups.

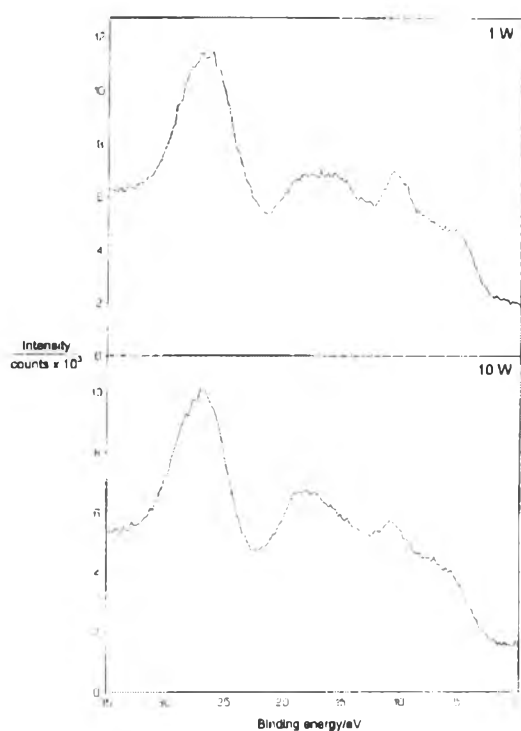


Figure 2.12 Valence-band XPS spectra of 1-W and 10-W plasma-polymerized acrylic acid.

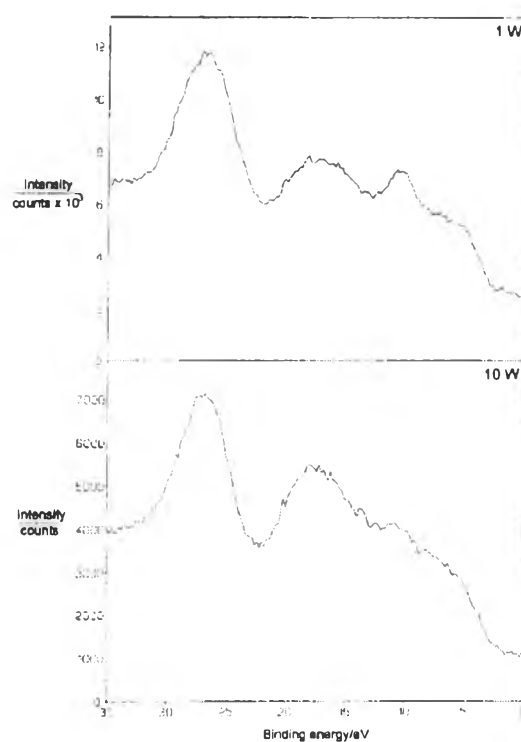


Figure 2.13 Valence-band XPS spectra of 1-W and 10-W plasma-polymerized propanoic acid.

2.5 Ethylene

Ethylene is a naturally produced, simple two carbon gaseous plant growth regulator that has numerous effects on the growth, development and storage life of many fruits, vegetables and ornamental crops. Both the synthesis and action of C_2H_4 involve complicated metabolic processes, which require oxygen and are sensitive to elevated concentrations of carbon dioxide. Plants produce C_2H_4 for climacteric ripening fruit and diseased or wounded tissue produce it in sufficient amounts to affect adjacent tissue. Sources of C_2H_4 not only include other plants (e.g. a ripe apple in a paper bag to promote the ripening of bananas), but also includes smoke, exhaust gases, compressed C_2H_4 gas, C_2H_4 releasing chemicals (e.g. ethephon), catalytic production of C_2H_4 from ethanol, and C_2H_4 analogues produced by a variety of processes (Abeles *et al.*, 1992).

Leon *et al.* (2006) studied development of new palladium promoted ethylene scavenger. A palladium (Pd) promoted the powder material that has significant ethylene adsorption capacity ($4162 \mu L g^{-1}$ material) at $20^\circ C$ and approximately 100% RH was identified and was shown to be far superior to $KMnO_4$ -based scavengers when used in low amounts and in conditions of high relative humidity (RH). Initial screening was carried out in a plug flow reactor with $200 \mu L L^{-1}$ ethylene, 10% (v/v) O_2 balanced with He at approximately 100% RH. The Pd-promoted material at either 0.01 or 0.03 g L^{-1} effectively scavenged both exogenously administered ($100 \mu L L^{-1}$) and/or endogenously produced ethylene by banana or avocado, respectively, to sub- $\mu L L^{-1}$ concentrations within a 24 h period. Optimum ethylene adsorption capacity was calculated as approximately $10,000 \mu L g^{-1}$. Accordingly, corresponding inhibition of ethylene-induced ripening was observed. When removed, Pd-material did not disrupt subsequent ripening. The results from their study demonstrate that Pd-promoted material has commercial potential.